Skyrmion crystals in pseudo-spin-1/2 Bose–Einstein condensates*

Zhang Cong(张 聪)[a], Guo Wen-An(郭文安)[a)b)], Feng Shi-Ping(冯世平)[a)] and Yang Shi-Jie(杨师杰)[a)b)†]

[a)] *Department of Physics, Beijing Normal University, Beijing* 100875, *China*

[b)] *State Key Laboratory of Theoretical Physics, Institute of Theoretical Physics, Chinese Academy of Sciences, Beijing* 100190, *China*

(Received 25 March 2013; revised manuscript received 14 June 2013)

Exact two-dimensional solutions are constructed for the pseudo-spin-1/2 Bose–Einstein condensates, which are described by the coupled nonlinear Gross–Pitaevskii equations where the intra- and inter-species coupling constants are assumed to be equal. The equations are decoupled by means of re-combinations of the nonlinear terms of the hyperfine states according to the spatial dimensions. The stationary solutions form various spin textures which are identified as skyrmion crystals. In a special case, a crystal of skyrmion–anti-skyrmion pairs is formed in the soliton limit.

Keywords: Gross–Pitaevskii equations, exact solutions, skyrmion crystals

PACS: 03.75.Mn, 03.75.Lm, 02.30.Ik, 67.30.he **DOI:** 10.1088/1674-1056/22/11/110308

1. Introduction

A skyrmion is a particle-like topologically nontrivial soliton,[1] which is studied in a variety of research fields, especially in the condensed matter physics, such as the quantum Hall effects,[2–6] the liquid crystals,[7] and the helical ferromagnets.[8–10] It is noted early that three-dimensional (3D) skyrmions have physical properties of baryons while two-dimensional (2D) skyrmions play an important role in condensed matter systems. In recent experiments, it has been demonstrated that the 2D skyrmion spontaneously appears as the ground state in the helical magnets[1] and in the quantum Hall systems at fillings slightly away from unity.

Since the experimental realization of quantized vortices in alkali atomic Bose–Einstein condensates (BECs), phenomena related to the internal degrees of freedom are appealing for the investigation of topological objects.[11–22] Furthermore, precise spin manipulation techniques have been developed to prepare the topological spin structures of interest and provide unique opportunities to study their stability and dynamics.[23–28] The skyrmion–skyrmion interaction may lead to the formation of a skyrme crystal. Meanwhile, the periodic skyrmion crystal configurations could be used to model the nuclear matter.[29–32] Such a state was recently observed in a neutron scattering experiment.[33]

In this paper, we attempt to seek exact stationary solutions to the 2D coupled nonlinear Gross–Pitaevskii equations (GPEs) which describe the pseudo-spin-1/2 BECs. The intra- and inter-species interactions are assumed to be equal and the system is exposed to a uniform external field. We propose a method to decouple the GPEs by re-combinations of the nonlinearity and the spatial dimensions. Periodic solutions are obtained, which are shown to form skyrmion crystals in the pseudo-spin representation. In Section 2, we describe the method. The main results are given in Section 3. Section 4 gives a brief summary.

2. Method

We consider a 2D pseudo-spin-1/2 BEC in a uniform external potential ($V(\boldsymbol{r}) = 0$). We assume that the intra- and inter-species interaction strengths are $\gamma_{11} = \gamma_{12} \equiv \gamma$ and the two component atoms have the same mass $m_1 = m_2 \equiv m$. The Hamiltonian then has the pseudospin SU(2) symmetry.[19] By adopting the units of $\hbar = m = 1$, the stationary GPEs for the mean-field order parameter $\Psi = (\psi_1, \psi_2)^{\mathrm{T}}$ are

$$\mu_j \psi_j(\boldsymbol{r}) = \left[-\frac{1}{2}\nabla^2 + \gamma(|\psi_1(\boldsymbol{r})|^2 + |\psi_2(\boldsymbol{r})|^2) \right] \psi_j(\boldsymbol{r}), \quad (1)$$

where μ_j ($j = 1, 2$) denote the chemical potentials. In order to solve the coupled Eqs. (1), we decompose the wave functions according to the dimensions as

$$\begin{cases} \psi_1(x,y) = X_1(x)Y(y) + \mathrm{i}X(x)Y_1(y), \\ \psi_2(x,y) = X_2(x)Y(y) + \mathrm{i}X(x)Y_2(y), \end{cases} \quad (2)$$

where $X_1(x)$, $X_2(x)$, $X(x)$ and $Y_1(y)$, $Y_2(y)$, $Y(y)$ are real functions of a single variable. By imposing the restrictions

$$\begin{cases} |X_1(x)|^2 + |X_2(x)|^2 = B_1^2, \\ |Y_1(y)|^2 + |Y_2(y)|^2 = B_2^2, \end{cases} \quad (3)$$

where B_1 and B_2 are real constants, the total density can be separated as

$$\rho(\boldsymbol{r}) = B_1^2 X^2(x) + B_2^2 Y^2(y). \quad (4)$$

Substituting Eq. (2) into Eqs. (1) and equaling the real and the imaginary parts respectively, we obtain a set of ordinary differential equations for $X(x)$ and $Y(x)$, which can be solved

*Project supported by the National Basic Research Program of China (Grant No. 2012CB821403) and the National Natural Science Foundation of China (Grant No.11175018).

†Corresponding author. E-mail: yangshijie@tsinghua.org.cn

© 2013 Chinese Physical Society and IOP Publishing Ltd

self-consistently by making use of the unique properties of the Jacobian elliptical functions.[34] The details are described in the next section.

According to the relations of three non-singular Jacobian elliptical functions, sn, cn, and dn, we construct three types of solutions to Eqs. (1). They exhibit periodic crystals of skyrmions or skyrmion–anti-skyrmion pairs. The periods of the wavefunctions are $k = 4jK(m)$, where $K(m)$ is the complete elliptic integral of the first kind with modulus $0 < m < 1$ and j is an integer denoting the number of periods.

3. Stationary solutions

3.1. Type A

We first consider the following form of solution:

$$\begin{cases} \psi_1(x,y) = A\mathrm{sn}(kx,m)\mathrm{cn}(ky,m) + \mathrm{i}B\mathrm{cn}(kx,m)\mathrm{sn}(ky,m), \\ \psi_2(x,y) = D\mathrm{cn}(kx,m)\mathrm{cn}(ky,m). \end{cases} \tag{5}$$

This wavefunction automatically satisfies the periodic boundary conditions in the x and y directions due to the properties of the Jacobian elliptical functions. By substituting Eq. (5) into the stationary Eqs. (1) and using the identities between the Jacobian elliptic functions, we obtain the relations

$$A^2 = B^2 = D^2/2, \tag{6}$$

$$\begin{cases} \mu_1 = k^2(2-3m^2)/2, \\ \mu_2 = k^2(1-2m^2), \end{cases} \tag{7}$$

$$\gamma = -\frac{k^2m^2}{A^2}. \tag{8}$$

From $\gamma < 0$, we note that this solution applies to the BEC with attractive interactions. The difference between the chemical potentials μ_i $(i = 1,2)$ of the two components can be induced by a Zeeman energy. The total number of atoms is related to the amplitude of the wavefunction by

$$N = \frac{2A^2}{m^2}\left[m^2 - 1 + \frac{E(m)}{K(m)}\right], \tag{9}$$

where $E(m)$ is the complete elliptic integral of the second kind.

Figures 1(a) and 1(b) display the checkerboard distributions of density of each hyperfine state for $A = 1$, $B = 1$, $D = \sqrt{2}$, $\gamma = -45.4681$, $\mu_1 = 113.6702$, $\mu_2 = 90.9361$, and $m = 0.5$. The phase of ψ_1 shown in Fig. 1(c) reveals a periodic vortex–anti-vortex pair structure. The phase difference implies a particle current density given by[34,35]

$$j = \frac{1}{2\mathrm{i}}\sum_{j=1,2}[\psi_j^*(\nabla\psi_j) - (\nabla\psi_j^*)\psi_j]. \tag{10}$$

Figure 1(d) displays the vortex–anti-vortex structure of the total particle current.

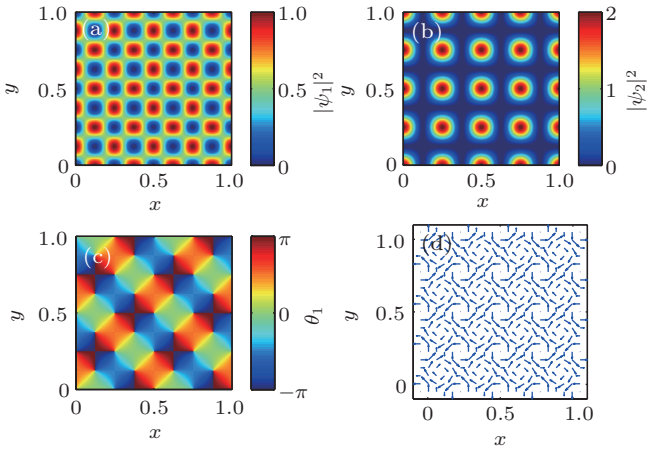


Fig. 1. (color online) The density profiles of hyperfine states (a) ψ_1 and (b) ψ_2 in state (5). The parameters are $A = 1$, $\gamma = -45.4681$, $\mu_1 = 113.6702$, $\mu_2 = 90.9361$, and $m = 0.5$. The two species have different particle numbers and different chemical potentials. (c) The phase distribution of the complex ψ_1 component. (d) The total particle current density. The number of periods in the wavefunction is $j = 2$.

In order to explore the topological structure of the state, we examine the normalized spinor $\boldsymbol{\chi}(\boldsymbol{r})$ which is defined by $\boldsymbol{\Psi}(\boldsymbol{r}) = \sqrt{\rho(\boldsymbol{r})}\boldsymbol{\chi}(\boldsymbol{r})$. The spin vector $\boldsymbol{S}$ for the condensates is $\boldsymbol{S}(\boldsymbol{r}) = \boldsymbol{\chi}^\dagger\boldsymbol{\sigma}\boldsymbol{\chi}$, with $\boldsymbol{\sigma}$ the Pauli matrices. Figure 2(a) displays the spin texture which forms a skyrmion crystal. The topological charge or the Pontryagian index of the skyrmion is an invariant[11]

$$Q = \int_{\mathrm{cell}} q(\boldsymbol{r})\,\mathrm{d}x\mathrm{d}y, \tag{11}$$

where the topological charge density is

$$q(\boldsymbol{r}) = \frac{1}{4\pi}\boldsymbol{S}\cdot(\partial_x\boldsymbol{S}\times\partial_y\boldsymbol{S}). \tag{12}$$

Figure 2(b) shows the distribution of $q(\boldsymbol{r})$, which exhibits a periodic structure. We note that in one period of state (5), there are four skyrmions. Each unit cell has a total topological charge $Q = 1$. The anti-skyrmion crystal can be obtained by simply taking the complex conjugate of state (5).

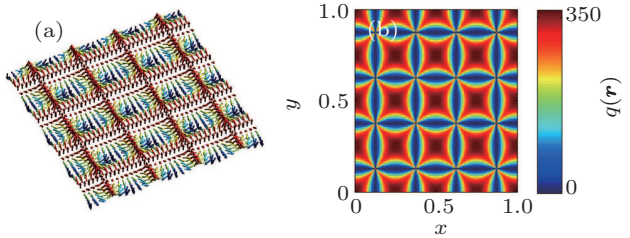


Fig. 2. (color online) (a) The spin texture $\boldsymbol{S}(\boldsymbol{r})$ of state (5) forms a skyrmion crystal. The number of periods is $j = 2$. (b) The distribution of the topological charge density $q(\boldsymbol{r})$. The total topological charge of each cell is unity.

3.2. Type B

Next we consider the solution for $\gamma > 0$, which is given by

$$\begin{cases} \psi_1(x,y) = A\mathrm{sn}(kx,m)\mathrm{cn}(ky,m) + \mathrm{i}B\mathrm{cn}(kx,m)\mathrm{sn}(ky,m), \\ \psi_2(x,y) = D\mathrm{sn}(kx,m)\mathrm{sn}(ky,m). \end{cases} \tag{13}$$

We obtain the relations

$$A^2 = B^2 = D^2/2, \tag{14}$$

$$\begin{cases} \mu_1 = k^2(2+m^2)/2, \\ \mu_2 = k^2(1+m^2), \end{cases} \tag{15}$$

$$\gamma = \frac{k^2 m^2}{A^2}. \tag{16}$$

The total number of atoms is related to the amplitude of the wavefunction by

$$N = \frac{2A^2}{m^2}\left[1 - \frac{E(m)}{K(m)}\right]. \tag{17}$$

Figure 3 displays the results for $j = 2$. The parameters are $A = 1$, $B = 1$, $D = \sqrt{2}$, $\gamma = 45.4681$, $\mu_1 = 204.6063$, $\mu_2 = 272.8084$, and $m = 0.5$. The spin texture forms a periodic crystal of anti-skyrmions as shown in Fig. 4(a). Our calculation shows that each anti-skyrmion has a total topological charge $Q = -1$ (Fig. 4(b)).

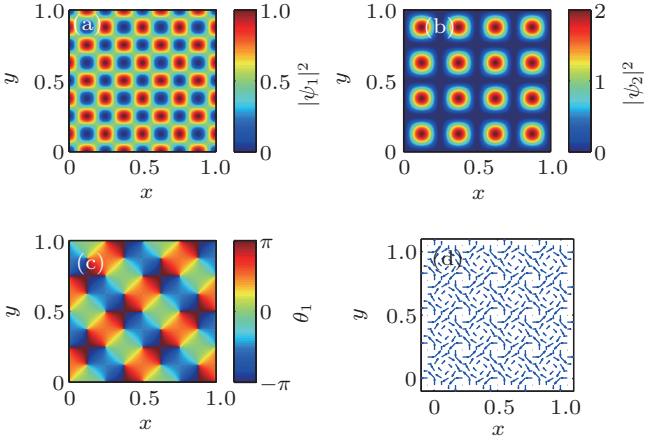


Fig. 3. (color online) The density profiles of hyperfine states (a) ψ_1 and (b) ψ_2 in state (13). (c) The phase distribution of the complex ψ_1 component. (d) The total particle current density. The parameters are $A = 1$, $\gamma = 45.4681$, $\mu_1 = 204.6063$, $\mu_2 = 272.8084$, and $m = 0.5$.

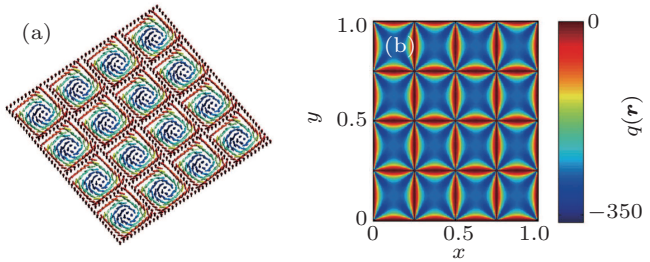


Fig. 4. (color online) (a) The spin texture $\boldsymbol{S}(\boldsymbol{r})$ of state (13). (b) The distribution of the topological charge density $q(\boldsymbol{r})$. The total topological charge in each cell is $Q = -1$.

3.3. Type C

We finally show an example of solution that is generally not a skyrmion for $m < 1$ while tending to be one in the soliton limit ($m \to 1$). The solution is of the form

$$\begin{cases} \psi_1(x,y) = A\mathrm{sn}(kx,m)\mathrm{dn}(ky,m) + \mathrm{i}B\mathrm{dn}(kx,m)\mathrm{sn}(ky,m), \\ \psi_2(x,y) = D\mathrm{dn}(kx,m)\mathrm{dn}(ky,m). \end{cases} \tag{18}$$

We obtain the relations

$$A^2 = B^2 = m^2 D^2/2, \tag{19}$$

$$\begin{cases} \mu_1 = k^2(2m^2-3)/2, \\ \mu_2 = k^2(m^2-2), \end{cases} \tag{20}$$

$$\gamma = -\frac{k^2}{A^2}. \tag{21}$$

Obviously, the solution applies to the attractive BECs. The total number of atoms is related to the amplitude of the wavefunction by

$$N = 2A^2\frac{E(m)}{K(m)}. \tag{22}$$

Figure 5 displays the results for state (18). The parameters are chosen as $A = 1$, $B = 1$, $D = \sqrt{2}$, $\gamma = -181.8723$, $\mu_1 = -227.3403$, $\mu_2 = -318.2765$, $m = 0.5$, and $j = 2$. Despite the similarity, state (18) is essentially distinct to the former two states. To clarify this point, we show in Fig. 6

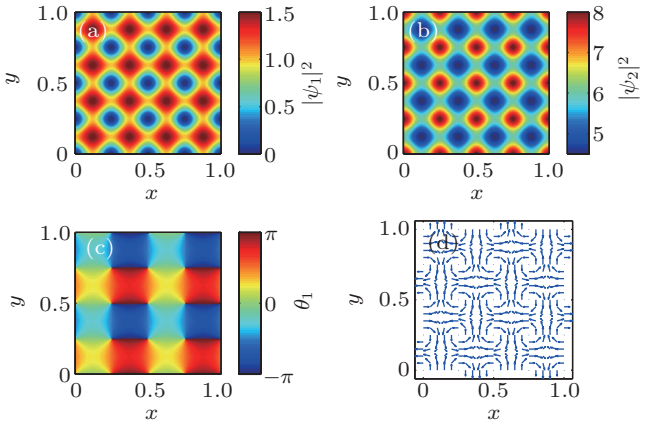


Fig. 5. (color online) The density profiles of hyperfine states (a) ψ_1 and (b) ψ_2 in state (18). (c) The phase distribution of the complex ψ_1 component. (d) The total particle current density. The parameters are $A = 1$, $\gamma = -181.8723$, $\mu_1 = -227.3403$, $\mu_2 = -318.2765$, and $m = 0.5$.

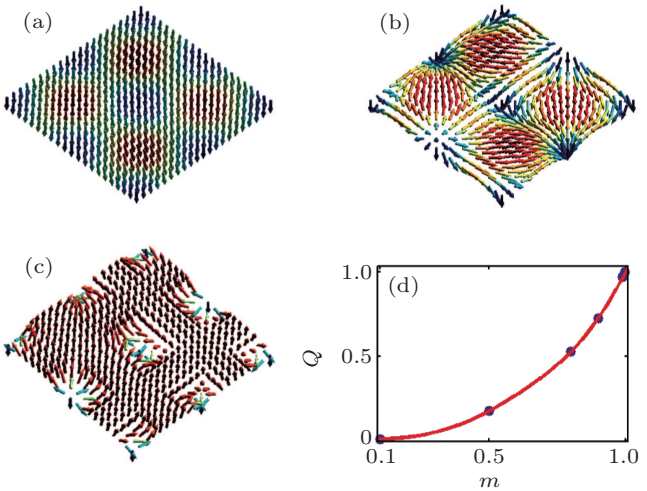


Fig. 6. (color online) The spin textures of state (18) for (a) $m = 0.1$, (b) $m = 0.8$, and (c) the solitonic limit $m = 0.999$. (d) The total charge defined by Eq. (11) versus modulus m. As $m \to 1$, the spin texture becomes a skyrmion–anti-skyrmion crystal.

the spin textures for various modulus m. We find that the total topological charge defined by Eq. (11) for each domain is not an integer. In a period, the spin texture does not form a skyrmion since the spin vector $\boldsymbol{S}(\boldsymbol{r})$ does not rotate a complete circle around the z axis, as shown in Figs. 6(a) and 6(b). Nevertheless, in the solitonic limit we find that the spin texture still forms a skyrmion–anti-skyrmion crystal in comparison to the former solutions. Figure 6(d) reveals that the total topological charge in each period is alternatively $Q = \pm 1$ as $m \to 1$. This configuration is shown in Fig. 7, where the charge density forms a dipole crystal.

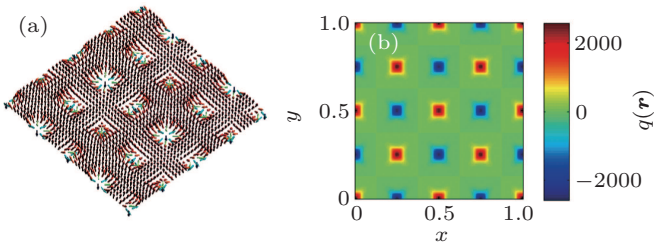


Fig. 7. (color online) (a) The spin texture $\boldsymbol{S}(\boldsymbol{r})$ of state (18) and (b) the distribution of the topological charge density $q(\boldsymbol{r})$ in the limit of $m \to 1$. The total topological charge in each cell is $Q = \pm 1$, which forms a dipole crystal.

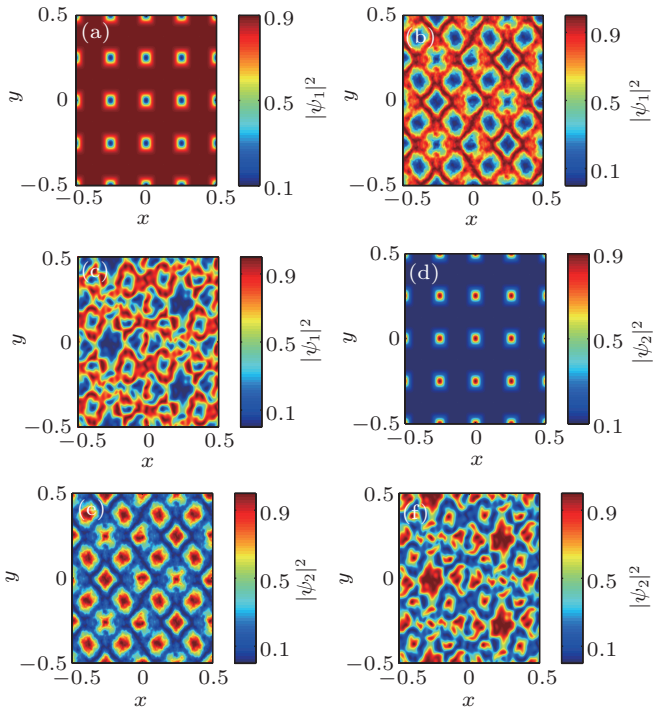


Fig. 8. (color online) The density distributions with the initial state being the skyrmion crystal state (5) in the limit of $m = 0.9999$ at the origin at: (a) and (d) $t = 0$, (b) and (e) $t = 0.005$, (c) and (f) $t = 0.01$. The particles transfer from the first component into the second one, and the skyrmion crystal annihilates correspondingly.

4. Numerical simulations

In order to examine the stability of these solutions, spatiotemporal evolutions are studied by numerically integrating the time-dependent GPEs.[37] A small periodical perturbation is applied to the evolution. We find that these states could survive a very short time when the Jacobian elliptical functions are under non-limit condition. As is known, solitons in 2D systems are normally stable. Thus, we consider the soliton limit of the solutions for the modulus $m \to 1$.

Selecting type A solution (5) as the initial state, we arrive at the changes of the density distribution in Fig. 8. The perturbation applied has the form $p = 0.001\sin(20kx)$. We identify that the skyrmion crystal in the soliton limit is still instable. Along the time, particles transfer from one component into the other, and the two components annihilate each other eventually.

We study the density distribution changes for the case with type B solution (13) as the initial state. In Fig. 9, we also obtain an unstable consequence.

Figure 10 shows the results for the case in which the initial state is the dipole crystal state (18). We note that the dipole crystal structure could be maintained until $t = 0.01$. Then more and more biases and collapses occur at the peaks of the density as time evolves, and the state annihilates finally.

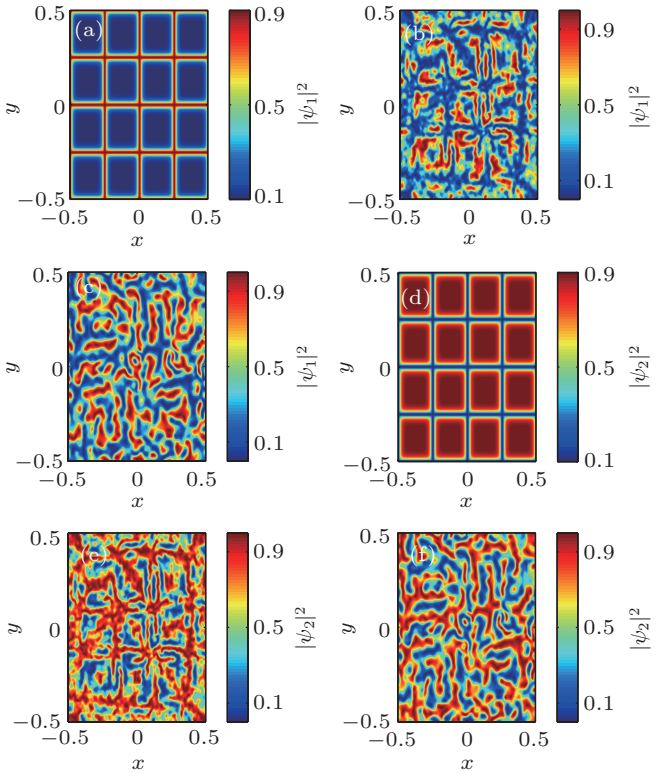


Fig. 9. (color online) The density distributions with the initial state being state (13) in the limit of $m = 0.9999$ at: (a) and (d) $t = 0$, (b) and (e) $t = 0.005$, (c) and (f) $t = 0.01$. The anti-skyrmion crystal gradually annihilates when $t \geq 0.005$.

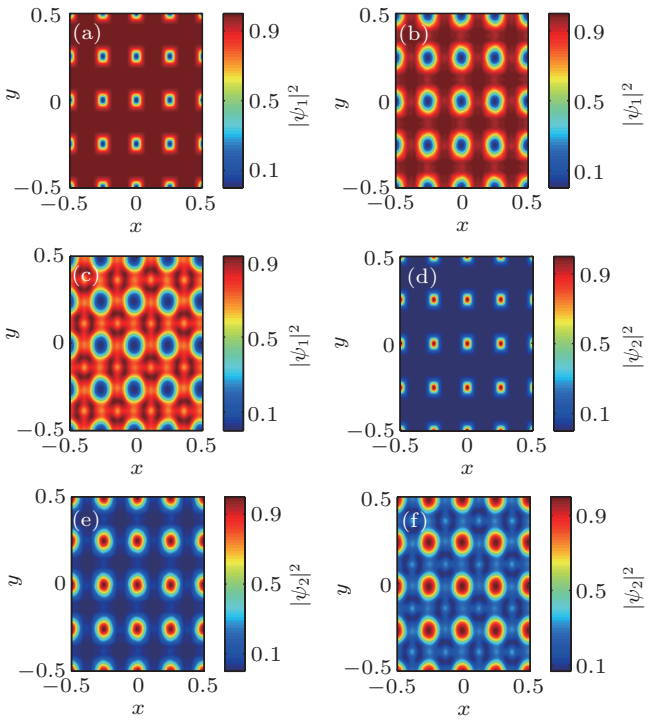


Fig. 10. (color online) The density distributions with the initial state being the dipole crystal state (18) in the limit of $m = 0.9999$ at: (a) and (d) $t = 0$, (b) and (e) $t = 0.005$, (c) and (f) $t = 0.01$. This state could survive for a brief time before annihilation.

In addition, we carry out the imaginary time evolution for the time-dependent GPEs to examine whether these analytical solutions are the ground states. When the evolving imaginary time is long enough ($t = 100$), we come upon the same stable states corresponding to the same interacting constants, which obviously prove that the stationary solutions constructed are not the ground states.

5. Summary

In summary, we have presented a class of exact solutions to the coupled GPEs which describe the pseudo-spin-1/2 BECs. The spin textures exhibit periodic crystals consisting of skyrmions ($Q = 1$ or $Q = -1$) or skyrmion–anti-skyrmion pairs. By real time evolving simulation, we have proved that the type C solution could survive for a brief time under the soliton limit, while other situations are unstable. We have also found that these lattice structure states are not the ground states of the system by imaginary time evolving simulation.

References

[1] Choi J Y, Kwon W J and Shin Y I 2012 *Phys. Rev. Lett.* **108** 035301
[2] Doucot B, Goerbig M O, Lederer P and Moessner R 2008 *Phys. Rev. B* **78** 195327
[3] Moon K, Mori H, Yang K, Girvin S M, MacDonald A H, Zheng L, Yoshioka D and Zhang S C 1995 *Phys. Rev. B* **51** 5138
[4] Sondhi S L, Karlhede A, Kivelson S A and Rezayi E H 1993 *Phys. Rev. B* **47** 16419
[5] Timm C, Girvin S M and Fertig H A 1998 *Phys. Rev. B* **58** 10634
[6] Schmeller A, Eisenstein J P, Pfeiffer L N and West K W 1995 *Phys. Rev. Lett.* **75** 4290
[7] Wright D C and Mermin N D 1989 *Rev. Mod. Phys.* **61** 385
[8] Zang J, Mostovoy M, Han J H and Nagaosa N 2011 *Phys. Rev. Lett.* **107** 136804
[9] Yu X Z, Onose Y, Kanazawa N, Park J H, Han J H, Matsui Y, Nagaosa N and Tokura Y 2010 *Nature* **465** 09124
[10] Neubauer A, Pfleiderer C, Binz B, Rosch A, Ritz R, Niklowitz P G and Böni P 2009 *Phys. Rev. Lett.* **102** 186602
[11] Yang S J, Wu Q S, Zhang S N and Feng S 2008 *Phys. Rev. A* **77** 033621
[12] Ramachandhran B, Opanchuk B, Liu X J, Pu H, Drummond P D and Hu H 2012 *Phys. Rev. A* **85** 023606
[13] Huhtamäki J A M and Kuopanportti P 2010 *Phys. Rev. A* **82** 053616
[14] Ruben G, Morgan M J and Paganin D M 2010 *Phys. Rev. Lett.* **105** 220402
[15] Huhtamäki J A M, Takahashi M, Simula T P, Mizushima T and Machida K 2010 *Phys. Rev. A* **81** 063623
[16] Scherer D R, Weiler C N, Neely T W and Anderson B P 2007 *Phys. Rev. Lett.* **98** 110402
[17] Liu C F, and Liu W M 2012 *Phys. Rev. A* **86** 033602
[18] Su S W, Liu I K, Tsai Y C, Liu W M and Gou S C 2012 *Phys. Rev. A* **86** 023601
[19] Kasamatsu K, Tsubota M and Ueda M 2005 *Phys. Rev. A* **71** 043611
[20] Kawakami T, Mizushima T, Nitta M and Machida K 2012 *Phys. Rev. Lett.* **109** 015301
[21] Li Y, Zhou X and Wu C 2012 arXiv:1205.2162
[22] Zhou X, Li Y, Cai Z and Wu C 2013 arXiv:1301.5403
[23] Bretin V, Rosenbusch P, Chevy F, Shlyapnikov G V and Dalibard J 2003 *Phys. Rev. Lett.* **90** 100403
[24] Schweikhard V, Coddington I, Engels P, Tung S and Cornell E A 2004 *Phys. Rev. Lett.* **93** 210403
[25] Zhang Y B, Mäkelä H and Suominen K A 2005 *Chin. Phys. Lett.* **22** 536
[26] Long C Y, Chen M L and Cai S H 2003 *Acta Phys. Sin.* **52** 1858 (in Chinese)
[27] Yu Z X, Liang J Q and Jiao Z Y 2004 *Chin. Phys. Lett.* **23** 8
[28] Leslie L S, Hansen A, Wright K C, Deutsch B M and Bigelow N P 2009 *Phys. Rev. Lett.* **103** 250401
[29] Skyrme T H R 1961 *Proc. R. Soc. A* **260** 127
[30] Skyrme T H R 1962 *Nucl. Phys.* **31** 556
[31] Klebanov I 1985 *Nucl. Phys. B* **262** 133
[32] Bogdanov A N and Yablonskii D A 1989 *Sov. Phys. JETP* **68** 101
[33] Mühlbauer S, Binz B, Joinetz F, Pfleiderer C, Rosch A, Neubauer A, Georgii R and Böni P 2009 *Science* **323** 915
[34] Abramowitz M and Stegun I A 1964 *Handbook of Mathematical Functions* (Washington, DC: National Bureau of Standards)
[35] Kasamatsu K, Tsubota M and Ueda M 2005 *Int. J. Mod. Phys. B* **19** 1835
[36] Ueda M and Kawaguchi Y 2012 *Phys. Reports* **520** 253
[37] Yang S J, Wu Q S, Feng S P, Wen Y C and Yu Y 2008 *Phys. Rev. A* **77** 035602